Quantum superposition states of Bose-Einstein condensates

J. I. Cirac,[1] M. Lewenstein,[2] K. Mølmer,[3] and P. Zoller[1]
[1]*Institut für Theoretische Physik, Universität Innsbruck, Technikerstrasse 25, A-6020 Innsbruck, Austria*
[2]*Commissariat a l'Enegie Atomique, DSM/DRECAM/SPAM, Centre d'Etudes de Saclay, 91191 Gif-sur-Yvette, France*
[3]*Institute of Physics and Astronomy, University of Aarhus, DK-8000 Århus C, Denmark*
(Received 16 June 1997)

We propose a scheme to create a macroscopic ''Schrödinger-cat'' state formed by two interacting Bose condensates. In analogy with *quantum optics*, where the control and engineering of quantum states can be maintained to a large extent, we consider the present scheme to be an example of *quantum atom optics* at work. [S1050-2947(98)06701-8]

PACS number(s): 03.75.Fi, 42.50.Fx, 32.80.−t

I. INTRODUCTION

The recent experimental realization of Bose-Einstein condensation of trapped cold rubidium [1], sodium [2], and lithium [3] atoms has initiated new areas of atomic, molecular and optical physics [4]. While some of these new areas remain still somewhat speculative, others have already attained firm experimental grounds and many of them are based on the analogy between the matter waves and electromagnetic waves or between bosonic atoms and photons.

On the level of single atoms, the analogy between the matter and electromagnetic waves has led to rapid developments of *atom optics* [5]. Some authors have thus considered the possibility of *nonlinear atom optics* in systems of many cold atoms, where the quantum statistical properties and atom-atom interactions become important [6]. It also has been pointed out [7] that nonlinear excitations of Bose-Einstein condensates (BECs) may lead to various analogs of nonlinear optics. Most of these theories have a mean-field character, i.e., they disregard quantum fluctuations of the atomic field operators and concentrate on the nonlinear Schrödinger-like wave equations for the matter wave functions.

In many situations, such as laser cooling or optical imaging, cold atoms not only exhibit their quantum statistical properties but they interact with photons. This fact motivated the developments of *quantum field theory of atoms and photons* [8]. Although this theory accounts in principle for quantum fluctuations of both atomic and electromagnetic fields, attention so far has been focused predominantly on the latter.

The atom-photon analogy has also triggered the studies in the area of the *physics of atom lasers* [9]. An atom laser, or a boser, is a matter wave analog of an ordinary laser. Quite recently, the possibility of employing BECs as a source of coherent matter waves has been demonstrated in the remarkable experiments of Andrews and co-workers [10].

We propose here to proceed with this analogy and look for the implementation of further elements of quantum optics in *quantum atom optics*. In our opinion, one of the major domains of concern of modern quantum optics is preparation, engineering, control, and detection of quantum states in various systems that involve light-matter interactions [11]. By analogy, quantum atom optics, in the sense proposed, concerns preparation, engineering, control, and detection of quantum states in atomic systems. Recent studies of excitations in trapped BECs belong to this category, although so far rather limited kinds of time-dependent perturbations of the trapping potential [12] have been used and only a few types of excitation have been investigated. Walsworth and You have proposed a method of selective creation of quasiparticle excitations in trapped BECs [13]. Their method, referred to as the spatial magnetic resonance method, could in principle allow for engineering and control of arbitrary excitation in the Bose-condensed system.

One of the most spectacular achievements of quantum optics in recent years has been the observation and study of macroscopic (or, strictly speaking, mesoscopic) ''Schrödinger-cat'' states of a trapped ion [14] and of an electromagnetic field in a high-Q cavity [15]. Schrödinger [16] introduced his famous ''cat'' states in order to illustrate the fundamental problem of the correspondence between the micro and macro worlds: the fact that quantum superposition states are never observed on the macro level. As postulated by von Neumann [17], this is due to irreversible reduction of superposition states into statistical mixtures. Such a reduction occurs in any quantum measurement process and leaves the system considered in a mixed state in a ''preferred'' basis, determined by the measurement. Modern quantum measurement theory [18] describes the reduction process in terms of quantum decoherence due to interactions of the system with environment [19]. Experimental realization of cat states thus requires typically sophisticated means to avoid the decoherence effects [14,15].

In this paper we demonstrate that it is feasible to prepare, control, and detect a Schrödinger cat formed by two interacting Bose condensates of atoms in different internal states. Atom-atom interactions in our model are mediated through atom-atom collisions and a Josephson-like laser coupling that interchanges internal atomic states in a coherent manner. The theory of such bicondensates restricted to collisional interactions only has been discussed recently in terms of the Thomas-Fermi approximation [20] and beyond [21,22]. Amazingly, the simultaneous condensation of ^{87}Rb atoms in two internal states $(F=2,M=2)$ and $(F=1,M=-1)$ has been recently achieved by Myatt *et al.* [23], using a combination of evaporative [24] and sympathetic [25] cooling. As pointed out by Julienne *et al.* [26], the simultaneous condensation was possible due to a very fortunate ratio of elastic to

inelastic collision rates for Rb atoms. For the moment, the prospects of extending the result of [23] to other atomic species are not promising. Nevertheless, one could expect that various ways of modifying atomic scattering lengths will be realized [27], which will allow one to control atomic collision processes in a desired way. The above comments apply to the case of magnetic traps. Once it becomes possible to achieve Bose-Einstein condensation in, for example, far-off-resonance traps, this will open other possibilities of trapping particles with different internal levels. This will allow one to meet in real atomic systems the conditions discussed below for the preparation of Schrödinger-cat states.

The plan of the paper is the following. In Sec. II we present the quantum field theoretical model of two trapped condensates and its simplified two-mode caricature. The detailed analysis of the two-mode model is carried out in Sec. III. We show that in some circumstances the ground state of the system becomes a Schrödinger cat and the system can be prepared in such a state by adiabatically changing the strength of the Josephson-like laser coupling. Various approximate solutions are tested here in comparison with the exact numerical solution of the problem. In Sec. IV approximate solutions of the complete quantum field theoretical model are found. They display the same qualitative behavior as the one obtained for the two-mode model. Finally, in Sec. V we discuss the feasibility of experimental observation of Schrödinger-cat states of two interacting Bose condensates.

II. QUANTUM FIELD THEORY OF TWO INTERACTING CONDENSATES

We consider here Bose-Einstein condensation of a trapped gas of atoms with two internal levels $|A\rangle$ and $|B\rangle$. The atoms interact via AA, BB, and AB elastic collisions. Additionally, a set of laser fields drives coherently a Raman transition connecting $|A\rangle \leftrightarrow |B\rangle$. In the formalism of second quantization, such a system is described by the Hamiltonian

$$H = H_A + H_B + H_{\rm int} + H_{\rm las}, \tag{1}$$

where

$$H_{A,B} = \int d^3\vec{x}\,\hat{\Psi}_{A,B}(\vec{x})^\dagger \Big[-\frac{\hbar^2}{2M}\nabla^2 + \frac{1}{2}M\omega_{A,B}^2 x^2 + \frac{4\pi\hbar^2 a_{A,B}^{\rm sc}}{2M}\,\hat{\Psi}_{A,B}(\vec{x})^\dagger \hat{\Psi}_{A,B}(\vec{x})\Big]\hat{\Psi}_{A,B}(\vec{x}), \tag{2a}$$

$$H_{\rm int} = \frac{4\pi\hbar^2 a_{AB}^{\rm sc}}{M}\int d^3\vec{x}\,\hat{\Psi}_A(\vec{x})^\dagger \hat{\Psi}_B(\vec{x})^\dagger \hat{\Psi}_B(\vec{x})\hat{\Psi}_A(\vec{x}), \tag{2b}$$

$$H_{\rm las} = -\frac{\hbar\Omega}{2}\int d^3\vec{x}\,[\hat{\Psi}_B(\vec{x})^\dagger \hat{\Psi}_A(\vec{x}) e^{-i\Delta t} + \hat{\Psi}_A(\vec{x})^\dagger \hat{\Psi}_B(\vec{x}) e^{+i\Delta t}]. \tag{2c}$$

Here $H_{A,B}$ describes the evolution of atoms in $|A\rangle$ and $|B\rangle$, respectively, in the absence of interactions between atoms in different internal states, $H_{\rm int}$ describes the interactions between atoms in $|A\rangle$ and $|B\rangle$ due to collisions, and $H_{\rm las}$ describes the Raman transitions induced by the laser detuned by Δ from the Raman resonance [28]; such interactions act as a Josephson-like coupling that transfers coherently particles between $|A\rangle$ and $|B\rangle$, at a Rabi frequency $\Omega > 0$. Atoms are confined in harmonic potentials of frequencies $\omega_{A,B}$, and $a_{A,B,AB}^{\rm sc}$ are the scattering lengths for the corresponding collisions, respectively. We assume that the collisions are purely elastic and that they do not change the number of particles in each internal level.

The field operators $\hat{\Psi}_{A,B}(\vec{x}), \hat{\Psi}_{A,B}(\vec{x})^\dagger$ annihilate and create atoms at $\vec{x}$ in the internal states $|A\rangle$ and $|B\rangle$. They fulfill the standard bosonic commutation relations

$$[\hat{\Psi}_A(\vec{x}), \hat{\Psi}_A(\vec{x}')^\dagger] = \delta(\vec{x}-\vec{x}'), \tag{3a}$$

$$[\hat{\Psi}_B(\vec{x}), \hat{\Psi}_B(\vec{x}')^\dagger] = \delta(\vec{x}-\vec{x}'). \tag{3b}$$

For the sake of simplicity, throughout this paper we will assume that $a_B^{\rm sc} = a_A^{\rm sc} \equiv a^{\rm sc}$, resonant laser excitation $\Delta = 0$, and $\omega_B = \omega_A \equiv \omega$. This makes the Hamiltonian (1) invariant under the exchange $A \leftrightarrow B$, which simplifies the analytical arguments. In experiment (cf. [23]) this symmetric situation is not directly realized since atoms in different (F,M) states experience different Zeeman effects in the magnetic field and thus ''feel'' different trap potentials. Nevertheless, we stress that our assumption has only a technical character. All the results presented below for the A-B symmetric case can be translated into the asymmetric case, as we shall see below. In general, if $\omega_A \neq \omega_B$, one can always choose the detuning $\Delta \neq 0$ to compensate for the potential difference. One should also mention that the different Zeeman effects, combined with gravity, may displace the traps with respect to each other; even for such a situation compensation of the potential difference using $\Delta \neq 0$ should be possible, although more complex.

Let us now rescale the variables to dimensionless ones as follows. First, we divide H by $\hbar\omega$ and then define $\lambda \equiv \Omega/2\omega > 0$, $\vec{r} \equiv \vec{x}/x_0$, $\hat{\Psi}(\vec{r}) \equiv \hat{\Psi}(\vec{x}) x_0^{3/2}$, $U_0 \equiv 4\pi a^{\rm sc}/x_0$, and $U_1 \equiv 4\pi a_{AB}^{\rm sc}/x_0$, where $x_0 \equiv (\hbar/M\omega)^{1/2}$. The rescaled dimensionless Hamiltonians (2) read now

$$H_{A,B} = \int d^3\vec{r}\,\hat{\Psi}_{A,B}(\vec{r})^\dagger \Big[-\frac{\nabla^2}{2} + \frac{r^2}{2} + \frac{U_0}{2}\,\hat{\Psi}_{A,B}(\vec{r})^\dagger \hat{\Psi}_{A,B}(\vec{r})\Big]\hat{\Psi}_{A,B}(\vec{r}), \tag{4a}$$

$$H_{\rm int} = U_1 \int d^3\vec{r}\,\hat{\Psi}_A(\vec{r})^\dagger \hat{\Psi}_B(\vec{r})^\dagger \hat{\Psi}_B(\vec{r})\hat{\Psi}_A(\vec{r}), \tag{4b}$$

$$H_{\rm las} = -\lambda \int d^3\vec{r}\,[\hat{\Psi}_B(\vec{r})^\dagger \hat{\Psi}_A(\vec{r}) + \hat{\Psi}_A(\vec{r})^\dagger \hat{\Psi}_B(\vec{r})]. \tag{4c}$$

Our objective is to study the properties of the system described by the above Hamiltonians at zero temperature. To this aim we need to find the ground state of the Hamiltonian (1) with the corresponding terms defined in Eqs. (4). The search for this state is a very difficult task. Under some conditions one can obtain mean-field approximations and nu-

merical (approximate) results for the ground state of Eq. (1). In order to understand better our model, we will first analyze a very simple two-mode model described by a caricature of the Hamiltonian (1). As we shall see in Secs. III and IV, the analysis of the simplified model resembles very much the analysis of the complete model described by Eq. (1).

The two-mode approximation of the Hamiltonian (1) is given by Eq. (1) but with

$$H_A=\omega_A a^\dagger a+\frac{U_{AA}}{2}a^\dagger a^\dagger a a, \tag{5a}$$

$$H_B=\omega_B b^\dagger b+\frac{U_{BB}}{2}b^\dagger b^\dagger b b, \tag{5b}$$

$$H_{\rm int}=U_1 a^\dagger b^\dagger b a, \tag{5c}$$

$$H_{\rm las}=-\lambda(a^\dagger b e^{-i\Delta t}+b^\dagger a e^{+i\Delta t}). \tag{5d}$$

This model corresponds to the previous one in the limit in which the external motion of the atoms is frozen. The bosonic annihilation and creation operators $a,a^\dagger$ and $b,b^\dagger$ annihilate and create atoms in internal states $|A\rangle$ and $|B\rangle$, respectively. They fulfill standard commutation relations $[a,a^\dagger]=[b,b^\dagger]=1$. As before, we will assume $\omega_B=\omega_A\equiv\omega$, $\Delta=0$, and $U_{AA}=U_{BB}\equiv U_0$. This allows us to neglect the first term in H_A and H_B since the total number of particles $N=a^\dagger a+b^\dagger b$ is conserved. Note that the same simplification occurs when $\omega_A\neq\omega_B$, but $\Delta=\omega_A-\omega_B$. This means that the results obtained in the next section for the A-B symmetric case are equivalent to the ones for the asymmetric case with appropriately chosen Δ.

An additional motivation behind the use of the model (5) is that it can be solved numerically for moderate N and therefore allows us to compare the analytical approximations with the exact numerical results. This will provide us with a guideline for the analysis of the complete quantum field theoretical model in the following section.

III. ANALYSIS OF THE TWO-MODE MODEL

In this section we consider in detail the simple two-mode model described by the Hamiltonians (5). The section is divided into three subsections. In Sec. III A we derive the ground-state energy of Eq. (5) using a mean-field approach, for which all the atoms are supposed to be in the same single-particle state. In Sec. III B we refine this theory to find a better approximation to the ground state. We show that under certain conditions the ground state corresponds to a *Schrödinger-cat state*. Finally, in Sec. III C we diagonalize the Hamiltonian exactly using a numerical method (5) and compare the exact predictions with the approximate ones of the previous subsections.

A. Mean-field approximation

The equations for the ground state in the mean-field (Hartree-like) approximation can be derived using the standard procedure. We consider the single-particle state

$$|\psi_1\rangle=\alpha_1|A\rangle+\beta_1|B\rangle, \tag{6}$$

where $|\alpha_1|^2+|\beta_1|^2=1$, and look for collective states of the N-particle system, with all the particles in the same state (6) that minimizes the total energy. Using the second quantization description, these collective states can be represented as

$$|\psi_N\rangle=|\psi_1\rangle\otimes|\psi_1\rangle\cdots|\psi_1\rangle=\frac{1}{\sqrt{N!}}[\alpha_1 a^\dagger+\beta_1 b^\dagger]^N|0\rangle, \tag{7}$$

where $|0\rangle$ denotes the vacuum state.

The expectation value of the Hamiltonian (5) in this state is

$$E(\alpha,\alpha^*,\beta,\beta^*)=\langle\psi_N|H|\psi_N\rangle=\frac{\widetilde{U}_0}{2}(|\alpha|^4+|\beta|^4)+\widetilde{U}_1|\alpha|^2|\beta|^2-\lambda(\alpha^*\beta+\beta^*\alpha), \tag{8}$$

where we have redefined $\widetilde{U}_{0,1}=U_{0,1}(N-1)/N$, and $\alpha=\sqrt{N}\alpha_1$ and $\beta=\sqrt{N}\beta_1$. The normalization condition imposes now

$$|\alpha|^2+|\beta|^2=N. \tag{9}$$

For simplicity of the notation, we will drop the tilde over U's in the following.

We minimize the mean energy (8) with respect to α,β and their complex conjugates, imposing the constraint (9) by using a Lagrange multiplier μ. After elementary calculations we obtain

$$[U_0|\alpha|^2+U_1|\beta|^2]\alpha-\lambda\beta=\mu\alpha, \tag{10a}$$

$$[U_0|\beta|^2+U_1|\alpha|^2]\beta-\lambda\alpha=\mu\beta. \tag{10b}$$

The above equations can be easily solved. To this aim, we first note that for $\lambda\neq0$, α and β can be taken to be nonvanishing real numbers. Thus we can divide Eq. (10a) by α and Eq. (10b) by β and subtract them to obtain

$$\left[U_1-U_0-\frac{\lambda}{\alpha\beta}\right](|\alpha|^2-|\beta|^2)=0. \tag{11}$$

The analysis of Eq. (11) is straightforward. Defining $\Lambda=2\lambda/[N(U_1-U_0)]$ one finds that for $|\Lambda|>1$ there exists only one solution

$$\alpha_0=\beta_0=\sqrt{N/2}, \tag{12}$$

which gives the mean energy (8)

$$E_0=\frac{N^2}{4}(U_0+U_1)-\lambda N. \tag{13}$$

For $|\Lambda|<1$ there exist three solutions $(0,+,-)$:

$$\alpha_0=\beta_0=\sqrt{N/2}, \tag{14a}$$

$$\alpha_\pm=\beta_\mp=\left[\frac{N}{2}(1\pm\sqrt{1-\Lambda^2})\right]^{1/2}, \tag{14b}$$

with the corresponding energies

$$E_0=\frac{N^2}{4}(U_0+U_1)-\lambda N, \tag{15a}$$

$$E_+=E_-=U_0\frac{N^2}{2}-\frac{\lambda^2}{U_1-U_0}. \tag{15b}$$

One can easily check that for $U_0>U_1$ we have $E_\pm>E_0$ and therefore the solution (α_0,β_0) gives the minimum energy. On the other hand, for $U_1>U_0$ both solutions (α_+,β_+) and (α_-,β_-) give a lower energy than (α_0,β_0) (in particular, for $\Lambda=1$, $E_0=E_\pm$).

The results can be summarized as follows. (a) For weak interactions between atoms in states $|A\rangle$ and $|B\rangle$, $U_0>U_1$ and the mean-field wave function for the ground state is

$$|\psi_N^0\rangle=\frac{1}{\sqrt{2^N N!}}[a^\dagger+b^\dagger]^N|0\rangle=\frac{1}{\sqrt{N^N N!}}[\alpha_0 a^\dagger+\beta_0 b^\dagger]^N|0\rangle. \tag{16}$$

(b) For strong interactions between atoms in states $|A\rangle$ and $|B\rangle$, $U_1>U_0$ and one has to distinguish two cases: (i) the strong laser case, in which $\Lambda\geqslant 1$ and the mean-field wave function is $|\psi_N^0\rangle$ given in Eq. (16), and (ii) the weak laser case, in which $\Lambda<1$ and there are two degenerate solutions $|\psi_N^\pm\rangle$ for the mean-field ground-state wave function

$$|\psi_N^\pm\rangle=\frac{1}{\sqrt{N^N N!}}[\alpha_\pm a^\dagger+\beta_\pm b^\dagger]^N|0\rangle, \tag{17}$$

where $\alpha_\pm$ and $\beta_\pm$ are given by expression (14b).

B. Beyond the mean-field approximation

For the chosen parameters, the Hamiltonian (1) with Eq. (5) is invariant under the operation T_{AB} that exchanges the internal level $|A\rangle$ with $|B\rangle$. Thus, in the case of no degeneracy the eigenstates of H, $|\phi_k\rangle$ must be eigenstates of T_{AB} too. Since T_{AB} is idempotent (i.e., has eigenvalues ± 1), the eigenstates have to fulfill $T_{AB}|\psi_k\rangle=\pm|\psi_k\rangle$. For $|\alpha|\neq|\beta|$ [case (ii) above], it is clear that the states obtained using the mean-field approach (7) do not satisfy this condition. This indicates that in case (ii) one can obtain a better approximation to the ground state with a lower energy if one uses as a variational ansatz the wave function

$$|\psi^\pm\rangle=(|\psi_N^+\rangle\pm|\psi_N^-\rangle)/\sqrt{2}. \tag{18}$$

This is a superposition of the two degenerate solutions. Note that $|\psi^\pm\rangle$ is indeed an eigenstate of T_{AB} with eigenvalue ± 1 and therefore it conforms with the symmetry of the Hamiltonian.

The states (18) are written as a superposition of two states in which all the atoms are in either the single-particle state $|\psi_1^+\rangle=\alpha_1^+|A\rangle+\beta_1^+|B\rangle$ or the single-particle state $|\psi_1^-\rangle=\alpha_1^-|A\rangle+\beta_1^-|B\rangle$. Therefore, they have the form of Schrödinger-cat states. Note, however, that a Schrödinger-cat state is characterized by its coherent inclusion of macroscopically distinguishable states. For the state of our condensates to be a true (i.e., macroscopic or at least mesoscopic) Schrödinger-cat state we must therefore require that the overlap ϵ,

$$\epsilon=\langle\psi_N^+|\psi_N^-\rangle=\Lambda^N, \tag{19}$$

be as small as possible. The ''size of the cat,'' which can be defined as $1/\epsilon$, should, on the other hand, be as large as possible. The theory should determine under which conditions the observation of the ''cat of maximal size'' is feasible.

The expectation value of the energy of the state (18) is

$$E_\pm=\frac{\langle\psi_N^+|H|\psi_N^+\rangle\pm\langle\psi_N^+|H|\psi_N^-\rangle}{1\pm\langle\psi_N^+|\psi_N^-\rangle}=\frac{N^2}{4}\frac{2U_0-\Lambda^2(U_1-U_0)\pm(\Lambda)^N(3U_0-U_1)}{1\pm(\Lambda)^N}. \tag{20}$$

It is easy to check that in the limit of $\epsilon\simeq 1$ (i.e., when the cat is still microscopic), we obtain

$$\Delta E=\frac{N}{2}(U_1-U_0). \tag{21}$$

This equation reveals characteristic scaling of the energy difference ΔE with N, which, as we shall see below, is also valid in the more interesting limit of $\epsilon=\Lambda^N\ll 1$ (i.e., when the cat is mesoscopic or macroscopic). In such case we may expand the result (20) first in ϵ and then in $N\gg 1$, so that we obtain

$$\Delta E=E_--E_+-\simeq\epsilon\ \ln(\epsilon)N(U_1-U_0). \tag{22}$$

Thus, for a ''given size'' of the cat $1/\epsilon$ the energy difference is proportional to N. Quite generally, the difficulty in cooling to a ground state of a *given* purity increases with an increasing number of atoms N, while a larger energy gap ΔE makes the cooling easier. In this sense, the scaling $\Delta E\propto N$ helps.

C. Exact numerical solution

In the Fock basis $|m\rangle_A\otimes|N-m\rangle_B$ $(m=0,1,\ldots,N)$ the Hamiltonian H is an $(N+1)\times(N+1)$ tridiagonal matrix and therefore can be easily diagonalized by numerical methods. Since the mean-field approximation and its improved version analyzed in the previous subsections should be valid in the limit $N\to\infty$, we concentrate here on the finite-N results.

Let us denote by

$$|\phi_k\rangle=\sum_{m=0}^{N}q_m^k|m\rangle_A\otimes|N-m\rangle_B \tag{23}$$

the eigenstate corresponding to the energy E_k $(k=0,1,\ldots,N$ and $E_0\leqslant E_1\leqslant\cdots<E_N)$. The results of our analysis are presented in Figs. 1–4. In Fig. 1 we have plotted the ground-state energy E_0 as a function of Λ for $N=1000$ and $U_1=3U_0$. Although this figure already shows the clear signatures of the ''phase transition'' to the Schrödinger-cat phase for $\Lambda<1$, it is more instructive to look at the relative behavior of the consecutive eigenenergies of the low excited states. This is represented in Fig. 2(a) for $N=1000$ and Fig. 2(b) for $N=10\,000$, where we have plotted the ratio between the energy difference of the first excited state and the ground state and the energy difference of the second and first excited states $(E_1-E_0)/(E_2-E_1)$, as a function of Λ for $U_1=3U_0$.

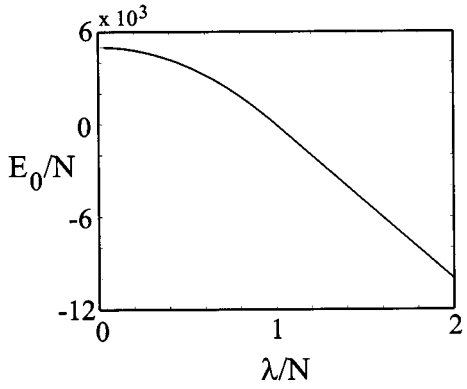

FIG. 1. Ground-state energy E_0 as a function of Λ for $N=1000$ and $U_1=3U_0$ calculated for the two-mode model. Note that according to the scalings, E_0 and λ are dimensionless.

The inset in Fig. 2(b) shows the magnification of the transition region. The figures clearly show that as Λ becomes smaller than 1, the energies of the first excited state and the ground state merge together. These two states become quasidegenerate, whereas the energy gap to the second excited state remains finite. Since the ground state is even and the first excited state is odd with respect to the A-B symmetry, and since they both are Schrödinger-cat states, their sum or difference describes the ''dead'' or ''alive cat,'' respectively.

In Figs. 3(a) and 3(b) we have plotted the energy of the first, second, and third excited states with respect to the energy of the ground state as a function of Λ for $N=1000$ and

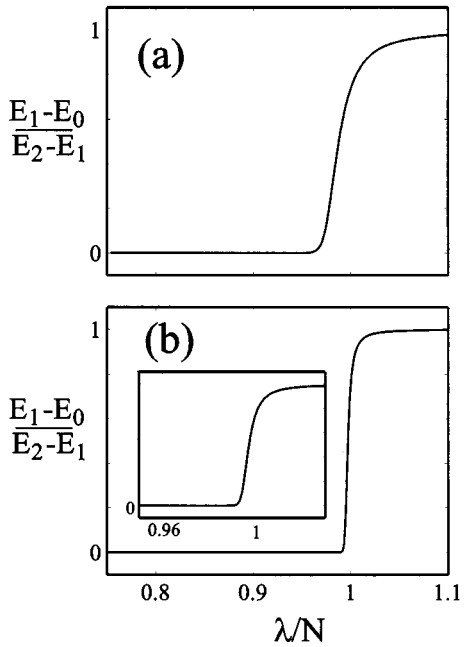

FIG. 2. (a) Ratio between the energy difference of the first excited state and the ground state, and the energy difference of the second and first excited states $(E_1-E_0)/(E_2-E_1)$, as a function of Λ for $U_1=3U_0$ and for $N=1000$. (b) Same as (a), but for $N=10\,000$. The inset shows the magnification of the transition region. The quantities plotted are dimensionless.

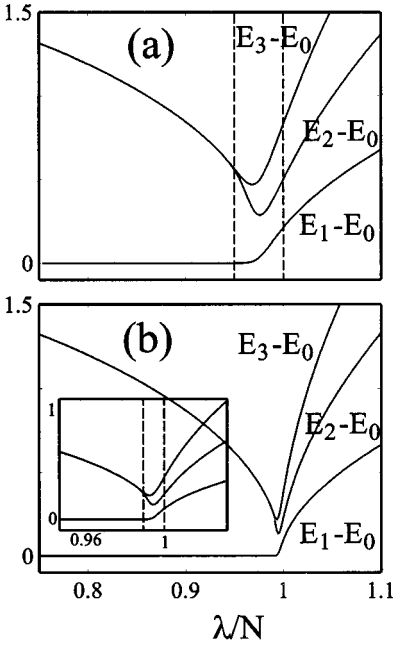

FIG. 3. (a) Energy of the first, second, and third excited states with respect to the energy of the ground state as a function of Λ for $N=1000$ and other parameters the same as in Fig. 1. The dashed lines mark approximately the transition region. (b) Same as (a), but for $N=10\,000$. The inset shows the magnification of the transition region. The quantities plotted are dimensionless.

$N=10\,000$, respectively. This figures clearly illustrate that, as expected, merging of the energy levels occurs not only for the two lowest ones but also within consecutive pairs of levels, i.e., E_3 becomes practically equal to E_2 for $\Lambda<1$, etc.

Finally, in Fig. 4 we have plotted the A-atom number distributions for the ground state [i.e., the coefficients $|q_m^0|^2$ from Eq. (23) as a function of m] for $N=1000$ [Fig. 4(a)] and $N=10\,000$ [Fig. 4(b)] for different values of Λ. These values belong to the transition regions between the dashed lines in Figs. 3(a) and 3(b).

The comparison of these results with the mean-field theory and its improved version is very satisfactory. Mean-field theory is practically exact outside of the transition region and gives errors of $O(1/N)$. The improved mean-field approximation of Sec. III B does a similar job for all values of the parameters, i.e., including the transition region. This result indicates that a similar improved mean-field approach can be used for the complete field theoretical model. We adopt this approach in Sec. IV.

Finally, the results indicate that due to the finite energy gap between the ground and first excited states it is possible to prepare and detect the Schrödinger-cat state in the following manner. Obviously, direct cooling of the system to the absolute ground state, which for $\Lambda<1$ is a cat state, would be a difficult task. The idea is therefore to first cool the system to a temperature T close to zero [i.e., such that $(E_1-E_0)/k_BT<1$] for $\Lambda>1$. Note that this is only possible in this regime of Λ since only there the first-excited-state energy is high enough so that practically all of the atoms can be cooled down to the ground state. Then we decrease $\Lambda(\lambda)$ adiabatically and enter the Schrödinger-cat phase: The system remains in the ground state, which now becomes the Schrödinger-cat state.

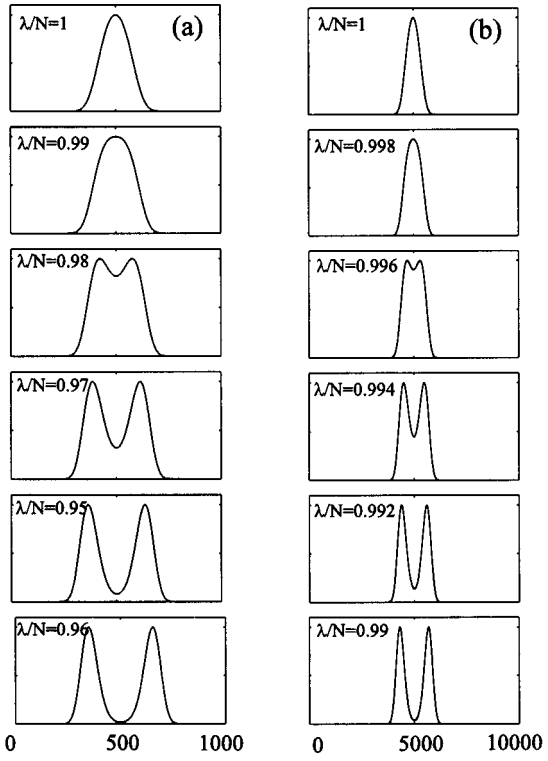

FIG. 4. (a) A-atom number distributions for the ground state [i.e., the coefficients $|q_m^0|^2$ from Eq. (23) as a function of m] for $N=1000$ for the values of Λ indicated. These values belong to the transition region between the dashed lines in Fig. 3(a). (b) Same as (a), but for $N=10\,000$. The values of Λ belong to the transition region between the dashed lines in Fig. 3(b). The quantities plotted are dimensionless.

Internal state-selective atom counting would then reveal a two-peaked structure corresponding to the $|\psi_N^{\pm}\rangle$ component. This, of course, would not prove the coherence. In the most general case, this would require tomographic techniques to reconstruct the complete density matrix of the two-mode system, similar to those developed for photon fields [31].

IV. ANALYSIS OF THE QUANTUM FIELD THEORETICAL MODEL

Here we analyze the full problem described by the Hamiltonians (1) and (4) that account for the atomic motional degrees of freedom. Given the similarities of this model to the two-mode model analyzed above, we follow steps similar to those in Sec. III. In Sec. IV A we apply the mean-field approximation to characterize the ground state of the full Hamiltonian. In principle, the exact solution of the mean-field equations is already very difficult to handle and requires numerical treatment. We have used instead two different methods to analyze it: the Thomas-Fermi approximation in Sec. IV B and the Gaussian variational ansatz for the single-particle wave function in Sec. IV C (for both methods cf. [30]). In both cases we find qualitatively the same results as for the two-mode model; in particular, in the strong-interaction and low-intensity limit [case (ii) above] there are two degenerate solutions of the mean-field equations. In Sec. IV D we go beyond the mean-field approximation to analyze these results. Finally, in Sec. IV E we utilize an even more sophisticated model to approximate numerically the eigenstates of the system.

A. Mean-field approximation

As in Sec. III A, we assume that the ground state of the system is a state for which all the atoms are in the same single-particle state

$$\langle \vec{r}|\psi_1\rangle = \alpha_1(\vec{r})|A\rangle + \beta_1(\vec{r})|B\rangle, \tag{24}$$

where

$$\int d^3\vec{r}[|\alpha_1(\vec{r})|^2 + |\beta_1(\vec{r})|^2] = 1. \tag{25}$$

The collective ground state of the whole system will then be, using the second quantization description,

$$|\psi_n\rangle = |\psi_1\rangle \otimes |\psi_1\rangle \cdots |\psi_1\rangle = \frac{1}{\sqrt{N!}}\left[\int d^3\vec{r}[\alpha_1(\vec{r})^* \hat{\Psi}_A(\vec{r})^\dagger + \beta_1(\vec{r})^* \hat{\Psi}_B(\vec{r})^\dagger]\right]^N |0\rangle, \tag{26}$$

where $|0\rangle$ denotes the vacuum state. The mean energy of this state can be easily calculated

$$\begin{aligned} E(\alpha,\alpha^*,\beta,\beta^*) &= \langle \psi_N|H|\psi_N\rangle \\ &= \frac{1}{2}\int d^3\vec{r}\,\alpha(\vec{r})^*\left[-\frac{\nabla^2}{2} + \frac{r^2}{2} + \frac{U_0}{2}|\alpha(\vec{r})|^2 + \frac{U_1}{2}|\beta(\vec{r})|^2\right]\alpha(\vec{r}) \\ &\quad - \frac{\lambda}{2}\int d^3\vec{r}[\alpha(\vec{r})^*\beta(\vec{r})\beta(\vec{r})^*\alpha(\vec{r})] \\ &\quad + (\alpha \leftrightarrow \beta). \end{aligned} \tag{27}$$

Here, as in the case of the two-mode system, we have defined $\tilde{U}_0 = U_0(N-1)/N$, $\tilde{U}_1 = U_1(N-1)/N$ (for simplicity we will omit the tilde in the following), $\alpha(\vec{r}) = \sqrt{N}\alpha_1(\vec{r})$, and $\beta(\vec{r}) = \sqrt{N}\beta_1(\vec{r})$. The normalization condition (25) becomes now

$$\int d^3\vec{r}[|\alpha(\vec{r})|^2 + |\beta(\vec{r})|^2] = N. \tag{28}$$

In Eq. (27) the expectation value of the energy is expressed as a functional of the single-particle wave functions $\alpha(\vec{r})$ and $\beta(\vec{r})$. The goal is now to minimize this energy with respect to these functions. In general, it is a difficult task that can be treated only numerically. In the following subsections we will follow two different approaches to find the solutions to this problem: first, we will analyze the Thomas-Fermi limit and second, we will use Gaussian ansatz.

B. Thomas-Fermi approximation

In order to minimize Eq. (27) we calculate the functional derivatives of the mean energy $E(\alpha,\alpha^*,\beta,\beta^*)$ with respect to α,β, and their complex conjugates using a Lagrange multiplier μ to ensure that the normalization condition (28) is fulfilled. This leads to a set of coupled nonlinear Schrödinger equations

$$\left[-\frac{\nabla^2}{2}+\frac{r^2}{2}+U_0|\alpha(\vec{r})|^2+U_1|\beta(\vec{r})|^2\right]\alpha(\vec{r})-\lambda\beta(\vec{r}) = \mu\alpha(\vec{r}), \tag{29a}$$

$$\left[-\frac{\nabla^2}{2}+\frac{r^2}{2}+U_0|\beta(\vec{r})|^2+U_1|\alpha(\vec{r})|^2\right]\beta(\vec{r})-\lambda\alpha(\vec{r}) = \mu\beta(\vec{r}). \tag{29b}$$

These equations are equivalent to Eqs. (10) for the two-level model. In the Thomas-Fermi approximation one assumes that the terms involving ∇^2 can be neglected in comparison to the interaction and potential terms.

According to Eqs. (29), for $\lambda\neq 0$, at any position $\vec{r}$, if $\beta(\vec{r})=0$ then $\alpha(\vec{r})=0$. This can be understood as follows. Consider, for example, that at some point $\alpha(\vec{r})\neq 0$ and $\beta(\vec{r})=0$; then the laser will take particles from state $|A\rangle$ to state $|B\rangle$, which will imply that $\beta(\vec{r})\neq 0$. This is not the case if $\lambda=0$, where displaced solutions in the Thomas-Fermi limit are indeed possible [20]. Thus we can concentrate on the positions $\vec{r}$, where $\alpha(\vec{r}),\beta(\vec{r})\neq 0$. Dividing Eqs. (29) by $\alpha(\vec{r})$ and $\beta(\vec{r})$, respectively, and taking the difference we find

$$\left[U_0-U_1+\frac{\lambda}{\alpha(\vec{r})\beta(\vec{r})}\right][|\alpha(\vec{r})|^2-\beta(\vec{r})|^2]=0, \tag{30}$$

which resembles very much Eq. (11). The analysis is, however, a bit more complicated. As before, there are two kinds of solutions $|\alpha(\vec{r})|=|\beta(\vec{r})|$ and $|\alpha(\vec{r})|\neq|\beta(\vec{r})|$, where the latter exists for sufficiently small λ only. In more detail, we can distinguish the following cases. (a) For a weak interactions between atoms in states $|A\rangle$ and $|B\rangle$, $U_0>U_1$ and the mean-field wave function for the ground state is Eq. (26) with

$$\alpha(\vec{r})=\beta(\vec{r})=\sqrt{\frac{1}{2(U_0+U_1)}(r_0^2-r^2)}, \tag{31}$$

where (for an isotropic trap in three dimensions)

$$r_0=\left[\frac{15}{8\pi}N(U_0+U_1)\right]^{1/5}. \tag{32}$$

(b) For strong interactions between atoms in states $|A\rangle$ and $|B\rangle$, $U_1>U_0$ and one has to distinguish two cases: (i) strong laser case, in which for

$$\Lambda\equiv\frac{2\lambda}{U_1-U_0}\geq\Lambda_0\equiv\left[\frac{15N}{8\pi}\right]^{2/5}(U_1+U_0)^{-3/5} \tag{33}$$

the mean-field ground-state wave function is the same as in case (a), and (ii) the weak laser case, in which for $\Lambda<\Lambda_0$ there exist two degenerate solutions $|\psi_N^{\pm}\rangle$ for the mean-field ground-state wave function of the form (26) with the coefficients $\alpha(\vec{r})$ and $\beta(\vec{r})$ given by

$$\alpha_{\pm}(\vec{r})^2=\beta_{\mp}(\vec{r})^2=\frac{1}{\sqrt{2}}[\rho_\mu(\vec{r})\pm\sqrt{\rho_\mu(\vec{r})^2-\Lambda^2}]^{1/2} \tag{34a}$$

for $r\leq r_1\equiv\sqrt{2(\mu-\Lambda U_0)}$ and

$$\alpha_+(\vec{r})=\alpha_-(\vec{r})=\frac{U_1-U_0}{U_1+U_0}[\rho_\mu(\vec{r})+\Lambda/2] \tag{34b}$$

for $r_2\equiv\sqrt{2\mu+(U_1-U_0)\Lambda}\geq r\geq r_1$, where $\rho_\mu(\vec{r})\equiv(\mu-r^2/2)/U_0$ and the value of the Lagrange multiplier μ has to be found by imposing the constraint (28).

Apart from numerical factors and different scalings, the Thomas-Fermi approximation gives results that are qualitatively similar to those found for the simple two-level model.

C. Gaussian variational ansatz

The Thomas-Fermi solution found in the preceding subsection is valid for $N\to\infty$ (or strictly speaking $NU_{0,1}\to\infty$) and predicts the existence of degenerate solutions for sufficiently low laser intensities. It is interesting to see if the effects remain for finite N. This can be analyzed using a Gaussian variational ansatz for the wave functions, i.e., setting

$$\alpha(\vec{r})=\sqrt{A}e^{-r^2/4a}, \tag{35a}$$

$$\beta(\vec{r})=\sqrt{B}e^{-r^2/4b}, \tag{35b}$$

with the variational parameters A,B,a,b. These parameters are not completely independent since the normalization (28) requires

$$N=(2\pi)^{3/2}(Aa^3+Bb^3). \tag{36}$$

Substituting this ansatz into Eq. (27), we find that the expectation value of the energy depends on the variational parameters a,A,b,B. We minimize it then with respect to those parameters taking into account the normalization condition (36). On the other hand, the stability analysis of these solutions can be performed very easily using the methods developed in [32].

We have not found analytical solutions in this case. However, we have solved the problem numerically and found the same qualitative results as in the Thomas-Fermi approximation. That is, in the case of weak interactions between atoms in states $|A\rangle$ and $|B\rangle$ $(U_0>U_1)$ there exists only one solution that corresponds to $A=B$ and $a=b$. In the case of strong interactions between atoms in the states $|A\rangle$ and $|B\rangle$ $(U_1>U_0)$, for a given number of particles N we find that there exists $\Lambda_0(N)$ such that if $\Lambda>\Lambda_0$ the minimum energy corresponds to the case $A=B$ and $a=b$ again; conversely, if $\Lambda\leq\Lambda_0$ there exist two solutions with $A\neq B$ and $a\neq b$. The stability analysis shows that these solutions are stable in all

these cases. The reason, as mentioned above, is that the laser beam tends to transfer the atoms that are pushed out of the condensate to the other internal level (see [22]).

D. Beyond the mean field

For our choice of parameters, the Hamiltonian (1) with Eq. (4) is invariant under the operation T_{AB} that exchanges the internal level $|A\rangle$ with $|B\rangle$. Thus the ground state of the Hamiltonian has to be an eigenstate of this operator. If we impose this condition on the ansatz (26) we find that $|\alpha(\vec{r})|=|\beta(\vec{r})|$. As we have seen in the preceding subsections [cases (ii)], for a given number of particles there exists a certain Λ_0 such that if $\Lambda<\Lambda_0$ there are two wave functions of the form (26) $|\psi_\pm\rangle$ with $\alpha_\pm(\vec{r})\neq\beta_\pm(\vec{r})$ that have lower energy than that given by the solution $|\alpha(\vec{r})|=|\beta(\vec{r})|$. This implies in turn that there exists a better variational ansatz to the problem, namely,

$$|\psi^\pm\rangle=|\psi_N^+\rangle\pm|\psi_N^-\rangle, \tag{37}$$

where

$$|\psi_N^\pm\rangle=\frac{1}{\sqrt{N!}}\left[\int d^3\vec{r}\,[\,\alpha_1^\pm(\vec{r})^*\hat{\Psi}_A(\vec{r})^\dagger+\beta_1^\pm(\vec{r})^*\hat{\Psi}_B(\vec{r})^\dagger]\right]^N, \tag{38}$$

The corresponding energy is given by

$$E_\pm=\frac{\langle\psi_N^-|H|\psi_N^+\rangle\pm\langle\psi_N^+|H|\psi_N^-\rangle}{1\pm\langle\psi_N^+|\psi_N^-\rangle}. \tag{39}$$

It can be easily checked that $E_+<\langle\psi_N^+|H|\psi_N^+\rangle<E_-$. Thus, similarly to the two-level model, the proper ground-state ansatz has the form of a Schrödinger-cat state.

E. Approximate numerical solution

It is possible to use an even more general ansatz to generate better approximations to the real ground state of the Hamiltonian (1). In that case no analytical approximation is possible and one has to restrict oneself to numerical evaluations. In any case, one can check whether the existence of Schrödinger-cat states is compatible with these more elaborate calculations and one may confirm the mean-field solutions. In the following we use the ansatz

$$|\hat{\Psi}\rangle=\sum_{m=0}^{N}\frac{q_m}{\sqrt{m!(N-m)!}}\left[\int d^3\vec{r}\;\alpha_m(\vec{r})\hat{\Psi}_a(\vec{r})^\dagger\right]^m \times\left[\int d^3\vec{r}\;\beta_{N-m}(\vec{r})\hat{\Psi}_b(\vec{r})^\dagger\right]^{N-m}|0\rangle, \tag{40}$$

where q_m's and the wave functions $\alpha_m(\vec{r})$ and $\beta_m(\vec{r})$ are the variational parameters. To conform to the symmetry of the full Hamiltonian we impose additionally that

$$\beta_m(\vec{r})=\alpha_m(\vec{r}),\quad q_m=q_{N-m}. \tag{41}$$

If the ansatz (40) is used to calculate the expectation value of the Hamiltonian $\langle\hat{\Psi}|H|\hat{\Psi}\rangle$, one finds a rather complicated expression involving the expansion coefficients q_m and the wave functions $\alpha_m(\vec{r})$: an infinite set of nonlinear Schrödinger equations that couples $q_m\rightarrow q_m, q_{m\pm1}$ as well as $\alpha_m\rightarrow\alpha_m,\alpha_{m\pm1},\alpha_{N-m},\alpha_{N-m\pm1}$. A solution of these equations seems to be an impossible task, but fortunately the equations simplify in the limit of sufficiently large N. We have proved using the systematic $1/\sqrt{N}$ expansion that in this limit one can simply substitute $m\simeq m\pm1$, which implies $\alpha_m\simeq\alpha_{m\pm1}$, as well as $q_m\simeq q_{m\pm1}$ in the equations for α_m's.

The resulting set of differential equations for $\alpha_m(\vec{r})$'s has the form

$$\left[-\frac{\nabla^2}{2}+\frac{r^2}{2}+U_0|\tilde{\alpha}_m(\vec{r})|^2+U_1|\tilde{\alpha}_{N-m}(\vec{r})|^2\right]\tilde{\alpha}_m(\vec{r}) -2\lambda\tilde{\alpha}_{N-m}(\vec{r})=\mu_m\tilde{\alpha}_m(\vec{r}), \tag{42}$$

where $\tilde{\alpha}_m(\vec{r})\equiv\sqrt{m}\,\alpha_m(\vec{r})$ and with μ_m such that the normalization condition

$$m=\int d^3\vec{r}\,|\tilde{\alpha}_m(\vec{r})|^2 \tag{43}$$

is fulfilled. The above equations have to be accompanied by the linear Schrödinger equations for q_m that contain tridiagonal coupling to $q_{m\pm1}$. The coefficients in the latter equations, however, depend functionally, in a highly nonlinear way, on the α_m's,

$$Eq_m=E_mq_m-\lambda L_mq_{m-1}-\lambda K_mq_{m+1}, \tag{44}$$

where E denotes the eigenvalue we search for, whereas

$$E_m=\frac{1}{2}\int d^3\vec{r}\;\alpha_m(\vec{r})^*\left[-\frac{\nabla^2}{2}+\frac{r^2}{2}+\frac{U_0}{2}|\alpha_m(\vec{r})|^2 +\frac{U_1}{2}|\alpha_{N-m}(\vec{r})|^2\right]\alpha_m(\vec{r})+(m\leftrightarrow N-m), \tag{45}$$

$$L_m=\sqrt{m(N-m+1)}\int d^3\vec{r}\;\alpha_{m-1}(\vec{r})^*\alpha_{N-m+1}(\vec{r}), \tag{46}$$

$$K_m=\sqrt{(m+1)(N-m)}\int d^3\vec{r}\;\alpha_{m+1}(\vec{r})^*\alpha_{N-m-1}(\vec{r}). \tag{47}$$

The coefficients q_m are normalized as

$$\sum_{m=0}^{N}|q_m|^2=1. \tag{48}$$

Note that Eq. (42) is similar to Eqs. (29) except the former takes fully into account the change of the form of the wave function with m. Unfortunately, these equations are still very difficult to solve, even using the Thomas-Fermi approximation. We can show, however, that the condition $\alpha_{N-m}(\vec{r})>\alpha_m(\vec{r})$ $(m<N/2)$ is fulfilled everywhere, a conclusion that could also be reached in the context of our

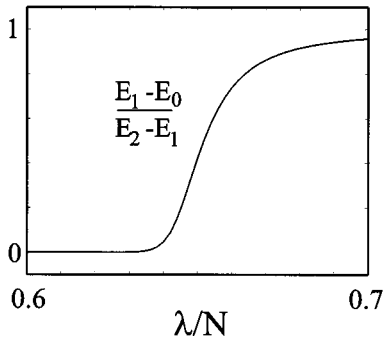

FIG. 5. Energy difference of the first excited state and the ground state, and the energy difference of the second and first excited states $(E_1-E_0)/(E_2-E_1)$, as a function of Λ for $N=1000$ and $U_1=3U_0$, calculated for the complete quantum field theoretical model. The parameters are $a_A^{sc}=a_B^{sc}=50$ nm, $a_{AB}^{sc}=150$ nm, $x_0=3$ μm, and $\hbar\omega=100$ Hz. The quantities plotted are dimensionless.

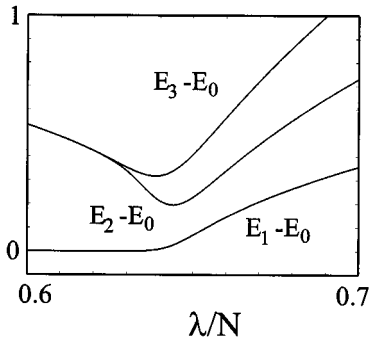

FIG. 6. Energy of the first, second, and third excited states with respect to the energy of the ground state as a function of Λ calculated for the complete quantum field theoretical model. The parameters are the same as in Fig. 5. The quantities plotted are dimensionless.

mean-field theory. Guided by this observation, we use simple Gaussian functions to approximate the solution of Eq. (42). In other words, we set

$$\alpha_m(\vec{r})=\sqrt{A_m}e^{-r^2/4a_m} \tag{49}$$

and minimize the mean-field energy numerically with respect to the a_m. Note that the normalization condition implies automatically that $m=A_m(2\pi a_m^2)^{3/2}$, so that the value of A_m is determined by the value of a_m. In an even more sophisticated attempt we have used as a variational ansatz a sum of two different Gaussians of the form (49). This calculation has led to practically the same results as the ones obtained with a single Gaussian ansatz. For this reason we present below numerical results corresponding to a single Gaussian ansatz.

Our main results are shown in Figs. 5 and 6. Figure 5 is the straightforward analog of Fig. 2(a). We have plotted there the ratio between the energy difference of the first excited state and the ground state and the energy difference of the second and first excited states $(E_1-E_0)/(E_2-E_1)$ as a function of Λ for $N=1000$ and $U_1=3U_0$. We have used the parameters $a_A^{sc}=a_B^{sc}=50$ nm, $a_{AB}^{sc}=150$ nm, $x_0=3$ μm, and $\hbar\omega=100$ Hz. The figure clearly shows that, as in the case of the two-mode model, as Λ becomes smaller than 1, the energies of the first excited state and the ground state merge together. These two states become quasidegenerate, whereas the energy gap to the second excited state remains finite.

Similarly, Fig. 6 is an analog of Fig. 3(a). There we have plotted the energy of the first, second, and third excited states with respect to the energy of the ground state as a function of Λ. As already seen in the two-mode model, merging of the energy levels occurs also among consecutive pairs of levels, i.e., E_3 becomes practically equal to E_2 for $\Lambda<1$.

In conclusion, we stress that the similarity between Figs. 2(a), 3(a), 5, and 6 is remarkable. Clearly, the complete field theoretical model leads to the same physics as the two-mode model. As Λ is adiabatically decreased, the system enters the Schrödinger-cat phase in which the ground state is a linear superposition of two states for which the A-atom number distributions are significantly distinct.

V. IS A SCHRÖDINGER-CAT STATE EXPERIMENTALLY FEASIBLE?

We conclude with a summary of requirements to observe Schrödinger cats in an experiment. While these necessary conditions to prepare and preserve catlike states are not fulfilled in the present generation of Bose-Einstein experiments [23], they might provide a guideline and motivation for future experimental work.

A. *A*-*B* symmetry

The calculations in the present paper assume an A-B symmetry. We believe that this assumption is mainly a technical point in the theoretical calculation, but discuss this now in more detail.

The choice of equal scattering length $a_A^{sc}=a_B^{sc}$ is reasonable and agrees with the recent theoretical calculations [26]. The assumption of equal trap frequencies $\omega_A=\omega_B$, however, is typically not fulfilled in magnetic traps since atoms in different internal states feel different (magnetic) potentials, but could be realized in principle in an optical dipole trap, where it is assumed that the two states have the same electron configuration, so that the far-off resonance lasers induce the same light shifts. Another way of achieving equal trap frequencies is to compensate for an asymmetry $\omega_A\neq\omega_B$ using an appropriately detuned laser. Such compensation is exact in the case of the two-mode model. In the case of the complete field theoretical model it requires a little more care. The idea is that the necessary and sufficient condition for a ground state of the system to be a Schrödinger-cat state is that there exist two distinct and degenerate minima of the energy in the mean-field approximation. If $\omega_A\neq\omega_B$ the mean-field theory would typically lead to two minima of the energy function, but with slightly different energies. The reader can easily convince himself or herself that this is the case for the two-mode model, while the analysis for the complete model is more technical, but otherwise analogous (especially in the Thomas-Fermi limit). This means that in such cases we would have one global and one local minimum of the energy and neither of them would correspond to a Schrödinger-cat state. They will, however, be characterized by different numbers of atoms in states $|A\rangle$ and $|B\rangle$. The

point is that the energies of these minima and the corresponding A- and B-atom numbers can be deformed in a continuous manner by changing Δ. At some point one arrives at the situation when the two minima become degenerate and at which the true ground state becomes a linear combination of the two, i.e., becomes a Schrödinger cat.

B. Instability condition $a_{AB}^{sc} > a_{A,B}^{sc}$

The existence of cat states imposes the (instability) condition $a_{AB}^{sc} > a_{A,B}^{sc}$ (i.e., $U_1 > U_0$). As we know, the present experiments [23] with Rb atoms allow for simultaneous evaporative and sympathetic cooling because the inelastic collision rates are small, which is directly related to the fact that $a_{AB}^{sc} \simeq a_A^{sc} \simeq a_B^{sc}$ [26]. While the condition seems not to be satisfied for atom species used in present *magnetic trap* experiments, we stress that future experiments might be based on different traps, for example, far-off-resonance traps using highly detuned laser light. This will open up the possibility of trapping new internal atomic states. Consider, for example, a total angular momentum $F=1$ and condensates in the states $m_F = \pm 1$. Furthermore, we assume that the level $m_F = 0$ does not participate in the collision dynamics (this can be done, for example, by shifting it with a laser). If the singlet scattering length is larger than the triplet scattering length, then the condition $a_{AB}^{sc} > a_{A,B}^{sc}$ will be fulfilled [29]. In addition, one can in principle modify the atom-atom scattering lengths using laser beams [27].

C. Cooling to the ground state

Preparation of a cat requires the cooling to the ground state of our system, i.e., the preparation of a *pure* state. The sufficient condition is that the temperature has to be $\kappa_B T \lesssim E_1$, where E_1 is the energy of the first excited state of the total Hamiltonian (for example, in the ideal case, that would require that approximately $N-1$ particles are in the ground state and one is in the first excited state). We stress that this requirement is much stronger than the requirement of having most of the atoms in the single-particle ground state, i.e., obtaining a *macroscopic occupation* of the ground state, as observed in current BEC experiments [1–3].

We illustrate this by an example. If we have N particles and 80% of them are in the ground state, the population of the collective ground state is only 0.8^N. Thus the temperatures required to observe a cat are much lower, such that practically all atoms are in the collective ground state. Whether existing cooling techniques, in particular evaporative cooling, can be extended into this regime remains to be investigated. However, the fact that we are dealing with bosons instead of distinguishable particles helps significantly to prepare a pure cat ground state. Consider a one-dimensional situation. For N distinguishable particles, there are N possible collective excited states with the same energy. Thus the temperature required to have most of the population in the collective ground state is $\kappa_B T \lesssim E_1/N$. On the contrary, for bosons this temperature is N *times higher*, $\kappa T \lesssim E_1$.

D. Decoherence

Finally, we should address the question of decoherence. Obviously, atom losses (such as those due to inelastic collisions) would destroy the Schrödinger-cat state very rapidly. In fact, in the extremal case when one has the cat $|0,N\rangle + |N,0\rangle$, already one atom loss would be enough to distort completely the coherent superposition (cf. [18,19,15]). We stress, however, that the situation here is similar to that of the experiment of Brune *et al.* [15]. The cats that live long enough to be observed must be mesoscopic. In fact, the Schrödinger-cat states displayed in Fig. 4 belong to that category. They allow for the loss of many atoms without the complete smearing out of their quantum-mechanical coherence. If they are created, they could allow for the study of the gradual decoherence process, in a manner similar to that in Ref. [15].

ACKNOWLEDGMENTS

We thank Y. Castin and H. Stoof for discussions. M. L. and K. M. thank J. I. Cirac and P. Zoller for hospitality extended to them during their visit to the University of Innsbruck. Work at the Institute for Theoretical Physics, University of Innsbruck was supported by the TMR network Grant No. ERBFMRX-CT96-0002 and the Österreichische Fonds zur Förderung der Wissenschaftlichen Forschung.

[1] M. H. Anderson, J. R. Ensher, M. R. Matthews, C. E. Wieman, and E. A. Cornell, Science **269**, 198 (1995).

[2] K. B. Davis, M.-O. Mewes, M. R. Andrews, N. J. van Druten, D. S. Durfee, D. M. Kurn, and W. Ketterle, Phys. Rev. Lett. **75**, 3969 (1995).

[3] C. C. Bradley, C. A. Sackett, and R. G. Hulet, Phys. Rev. Lett. **78**, 985 (1997).

[4] For a review see *Bose-Einstein Condensation*, edited by A. Griffin, D. W. Snoke, and S. Stringari (Cambridge University Press, New York, 1995).

[5] For a review see Appl. Phys. B: Photophys. Laser Chem. **54**, 5 (1992), special issue on optics and interferometry with atoms, edited by J. Mlynek, V. Balykin, and P. Meystre.

[6] G. Lenz, P. Meystre, and E. M. Wright, Phys. Rev. Lett. **71**, 3271 (1993); W. Zhang, D. F. Walls, and B. C. Sanders, *ibid.* **72**, 60 (1994).

[7] M. Edwards, P. A. Ruprecht, K. Burnett, P. J. Dodd, and C. W. Clark, Phys. Rev. Lett. **77**, 1671 (1997).

[8] For a review see M. Lewenstein and L. You, Adv. At., Mol., Opt. Phys. **36**, 221 (1996).

[9] Ch. J. Bordé, Phys. Lett. A **204**, 217 (1995); H. M. Wiseman and M. J. Collet, *ibid.* **202**, 246 (1995); R. J. C. Spreeuw, T. Pfau, U. Janicke, and M. Wilkens, Europhys. Lett. **32**, 469 (1995); M. Holland, K. Burnett, C. Gardiner, J. I. Cirac, and P. Zoller, Phys. Rev. A **54**, R1757 (1996); M. Olshan'ii, Y. Castin, and J. Dalibard, in *Proceedings of the 12th International*

Conference on Laser Spectroscopy, edited by M. Ignuscio, M. Allegrini, and A. Lasso (World Scientific, Singapore, 1995).
[10] M.-O. Mewes, M. R. Andrews, D. M. Kurn, D. S. Durfee, C. G. Townsend, and W. Ketterle, Phys. Rev. Lett. **78**, 582 (1997); M. R. Andrews, C. G. Townsend, H.-J. Miesner, D. S. Durfee, D. M. Kurn, and W. Ketterle, Science **275**, 637 (1997).
[11] J. F. Poyatos, J. I. Cirac, and P. Zoller, Phys. Rev. Lett. **77**, 4728 (1996).
[12] D. S. Jin, J. R. Ensher, M. R. Matthews, C. E. Wieman, and E. A. Cornell, Phys. Rev. Lett. **77**, 420 (1996); M.-O. Mewes, M. R. Andrews, N. J. van Druten, D. M. Kurn, D. S. Durfee, C. G. Townsend, and W. Ketterle, *ibid.* **77**, 988 (1996).
[13] R. Walsworth and L. You, Phys. Rev. A **56**, 555 (1997).
[14] C. Monroe, D. M. Meekhof, B. E. King, and D. J. Wineland, Science **272**, 1131 (1996).
[15] M. Brune, E. Hagley, J. Dreyer, X. Maître, A. Maali, C. Wunderlich, J. M. Raimond, and S. Haroche, Phys. Rev. Lett. **77**, 4887 (1996).
[16] E. Schrödinger, Naturwissenschaften **23**, 807 (1935); **23**, 823 (1935); **23**, 844 (1935).
[17] J. von Neumann, *Mathematische Grundlagen der Quantenmechanik* (Springer, Berlin, 1932).
[18] J. A. Wheeler and W. H. Żurek, *Quantum Theory and Measurement* (Princeton University Press, Princeton, 1983).
[19] W. H. Żurek, Phys. Today **44** (10), 36 (1991); W. H. Żurek, Phys. Rev. D **24**, 1516 (1981); **26**, 1862 (1982); A. O. Caldeira and A. J. Leggett, Physica A **121**, 587 (1983); E. Joos and H. D. Zeh, Z. Phys. B **59**, 223 (1985); R. Omnès, *The Interpretation of Quantum Mechanics* (Princeton University Press, Princeton, 1994).
[20] T.-L. Ho and V. B. Shenoy, Phys. Rev. Lett. **77**, 3276 (1996).
[21] B. D. Esry and C. H. Greene (unpublished).
[22] T. Busch, J. I. Cirac, V. Garcia-Perez, and P. Zoller, Phys. Rev. A **56**, 2978 (1997).
[23] C. J. Myatt, E. A. Burt, R. W. Ghrist, E. A. Cornell, and C. E. Wieman, Phys. Rev. Lett. **78**, 586 (1997).
[24] For a review see W. Ketterle and N. J. van Druten, Adv. At., Mol., Opt. Phys. **37**, 181 (1996).
[25] See, for instance, M. Lewenstein, J. I. Cirac, and P. Zoller, Phys. Rev. A **51**, 4617 (1995), and references cited therein.
[26] P. S. Julienne, F. H. Mies, E. Tiesinga, and C. J. Williams, Phys. Rev. Lett. **78**, 1880 (1997); see also J. P. Burke, Jr., J. L. Bohn, B. D. Esry, and C. H. Greene, Phys. Rev. A **55**, R2511 (1997).
[27] P. O. Fedichev, Yu. Kagan, G. V. Shlyapnikov, and J. T. M. Walraven, Phys. Rev. Lett. **77**, 2913 (1996), and references cited therein.
[28] For the coherent interaction of light and condensates see, for example, H. Zeng, W. Zhang, and F. Lin, Phys. Rev. A **52**, 2155 (1995); W. Zhang, Phys. Lett. A **176**, 225 (1993); W. Zhang and D. F. Walls, Phys. Rev. A **49**, 3799 (1994); **52**, 4696 (1995).
[29] H. Stoof (private communication).
[30] G. Baym and C. J. Pethick, Phys. Rev. Lett. **76**, 6 (1996).
[31] R. Walser (unpublished); E. L. Bolda, S. M. Tan, and D. F. Walls, quant-ph/9703014.
[32] For the stability study using a Gaussian ansatz see, for example, V. Pérez-Garcia, H. Michinal, J. I. Cirac, M. Lewenstein, and P. Zoller, Phys. Rev. Lett. **77**, 5320 (1996); for the stability with two condensates see Ref. [22].